Normalized water-leaving radiance: revisiting the influence of surface roughness

Howard R. Gordon

Many spaceborne sensors have been deployed to image the ocean in the visible portion of the spectrum. Information regarding the concentration of water constituents is contained in the water-leaving radiance—the radiance that is backscattered out of the water and subsequently propagates to the top of the atmosphere. Recognizing that it depends on the viewing and Sun geometry, ways have been sought to normalize this radiance to a single Sun-viewing geometry—forming the normalized water-leaving radiance. This requires understanding both the bidirectional nature of the upwelling radiance just beneath the surface and the interaction of this radiance with the air–water interface. I believe that the latter has been incorrectly computed in the past when a water surface roughened by the wind is considered. The presented computation suggests that, for wind speeds as high as 20 m/s, the influence of surface roughness is small for a wide range of Sun-viewing geometries, i.e., the transmittance of the (whitecap-free) air–water interface is nearly identical (within 0.01) to that for a flat interface.

OCIS codes: 010.4450, 280.0280, 240.5770, 290.4210.

1. Introduction

Many spaceborne sensors have been deployed to image the ocean in the visible portion of the spectrum. Their purpose has been to assess the concentration and variability of phytoplankton—the first link in the marine food chain. The information regarding the concentration (and that of other water constituents) is contained in the water-leaving radiance—the radiance that is backscattered out of the water and propagates to the top of the atmosphere. This radiance is typically less than 10% of the total measured at the sensor in the blue, and significantly less in the green and red. Recognizing that it depends on the viewing and Sun geometry, ways have been sought to normalize this radiance to a single Sun-viewing geometry—forming the normalized water-leaving radiance. This requires understanding both the bidirectional nature of the upwelling radiance just beneath the surface and the interaction of this radiance with the air–water interface. I believe that the latter has been incorrectly computed in the past for that portion of the water surface that is whitecap free. The correct computation is the subject of this paper.

I begin by reviewing the development of the normalized water-leaving radiance. Next, with the help of the reciprocity principle, I provide the details of computing the transmission through the wind-roughened air–water interface. Finally, I show that for solar zenith and sensor-viewing angles less than 60°, the influence of surface roughness is significantly less than described heretofore. In Appendix A I provide André Morel's corroboration of the conclusions reached in this paper.

2. Normalized Water-Leaving Radiance

The normalized water-leaving radiance $[L_w]_N$ was defined by Gordon and Clark[1] through

$$L_w(\lambda) = a_\oplus^{-2}[L_w(\lambda)]_N \cos\theta_s \exp\left\{-\left[\frac{\tau_R(\lambda)}{2} + \tau_{Oz}(\lambda)\right]\left(\frac{1}{\cos\theta_s}\right)\right\}, \quad (1)$$

where $L_w(\lambda)$ is the upward radiance at a wavelength λ just above the water surface that was backscattered out of the water; $\tau_R(\lambda)$ and $\tau_{Oz}(\lambda)$ are the optical thicknesses of the atmosphere associated with molecular (Rayleigh) scattering and ozone absorption, respectively; and $a_\oplus$ is the Earth–Sun distance in astronom-

The author is with the Department of Physics, University of Miami, Coral Gables, Florida 33124. His e-mail address is gordon@physics.miami.edu.

Received 2 July 2004; accepted 20 August 2004.
0003-6935/05/020241-08$15.00/0

ical units (AU). θ_s is the solar zenith angle. The exponential factor approximately accounts for the attenuation of solar irradiance from the top of the atmosphere to the water surface (approximately because the influence of aerosols is ignored). The cos θ_s factor is to reference the extraterrestrial solar irradiance to a horizontal surface rather than to the usual surface perpendicular to the solar beam. The $a_\oplus$ factor accounts for variations in $L_w(\lambda)$ that result from the eccentricity of the Earth's orbit about the Sun. The resulting normalized water-leaving radiance should depend mostly on the optical properties of the water and the roughness of the air–water interface. It is defined to approximate the radiance that would exit the ocean in the absence of the atmosphere, with the Sun at the zenith, at the mean Earth–Sun distance (1 AU). That radiance was given by Gordon and Clark[1] as

$$[L_w(\lambda)]_N = \overline{F}_0 \left[\frac{(1-\rho_f)(1-\overline{\rho}_f)}{m^2} \right] \frac{R}{Q}, \tag{2}$$

where $\overline{F}_0$ is the extraterrestrial solar irradiance for $a_\oplus = 1$ AU; $\overline{\rho}_f$ is the Fresnel reflectivity for the irradiance incident on the water surface from the Sun alone as there is no sky in the absence of the atmosphere [$(1 - \overline{\rho}_f)$ is the transmittance for the irradiance]; ρ_f is the reflectance of the air–water interface from below for radiance propagating toward the zenith [$(1 - \rho_f)$ is the transmittance for in-water radiance propagating toward the zenith]; R is the irradiance reflectance of the water just beneath the surface ($R = E_u/E_d$, where E_u and E_d are the upwelling and downwelling irradiances just beneath the water surface, respectively); and m is the refractive index of water. The quantity Q is the so-called Q factor defined as the upwelling irradiance just beneath the water surface E_u divided by the zenith-propagating upwelling radiance L_u just beneath the surface. Later, Gordon *et al.*[2] revised this to include multiple reflections within the water from the interface, i.e.,

$$[L_w(\lambda)]_N = \overline{F}_0 \left[\frac{(1-\rho_f)(1-\overline{\rho}_f)}{m^2(1-\overline{r}R)} \right] \frac{R}{Q}, \tag{3}$$

where $\overline{r}$ is the reflectance of upward irradiance by the interface, i.e., the reflected component of the downward irradiance is $\overline{r}E_u$. When the upwelling irradiance is totally diffuse (i.e., independent of the upward direction), the value of $\overline{r}$ is approximately[3] 0.48. These relations make no assumption regarding the uniformity or nonuniformity of the upwelling light field. Nonuniformity in the angular distribution of upwelling radiance is manifest in Q and $\overline{r}$; however, the contribution of the term containing $\overline{r}$ is small because R is usually <0.1, so the nonuniformity influence on $\overline{r}$ can be neglected.

In a series of papers, Morel and co-workers[4–8] have studied the angular distribution of upwelling radiance just beneath a water surface. Recognizing that spaceborne ocean color sensors are not limited to viewing only zenith-propagating radiance, and that the Sun is not necessarily at the zenith, they have defined normalized water-leaving radiance for the particular remote-sensing viewing geometry. Consider sunlight propagating toward the water in a direction specified by the unit vector $\hat{\xi}_s$ (Fig. 1). This is refracted into the water in a direction specified by $\hat{\xi}_s'$, resulting in upwelling radiance $L_u(\xi_v', \lambda)$ propagating in the direction $\hat{\xi}_v'$. This radiance is then propagated across the interface in a direction $\hat{\xi}_v$ forming the water-leaving radiance $L_w(\hat{\xi}_v, \lambda)$. The newer definition is

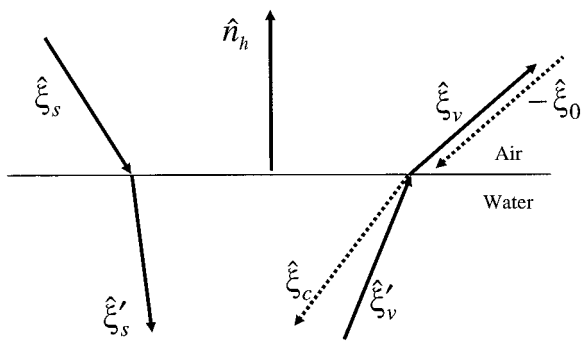

Fig. 1. Definitions of the unit vectors used in the text to describe the direction of propagation of various rays, along with the surface normal.

$$[L_w(\hat{\xi}_v)]_N = \overline{F}_0 \left\{ \frac{[1-\rho_f(\hat{\xi}_v')][1-\overline{\rho}_f(\hat{\xi}_s)]}{m^2[1-\overline{r}R(\hat{\xi}_s)]} \right\} \frac{R(\hat{\xi}_s)}{Q(\hat{\xi}_v', \hat{\xi}_s)}, \tag{4}$$

where λ was dropped from the argument list to simplify the notation. The term in the braces has been referred to by Morel and Gentili[7] as $\Re(\hat{\xi}_v', \hat{\xi}_s)$, i.e.,

$$\Re(\hat{\xi}_v', \hat{\xi}_s) = \left\{ \frac{[1-\rho_f(\hat{\xi}_v')][1-\overline{\rho}_f(\hat{\xi}_s)]}{m^2[1-\overline{r}R(\hat{\xi}_s)]} \right\}. \tag{5}$$

With the exception of $\overline{r}R(\hat{\xi}_s)$ in the denominator, this term depends solely on the reflection–transmission properties of the air–sea interface.

There are three important normalized water-leaving radiances that have been defined by Morel and Gentili.[7] The first is that of Gordon and Clark[1]: the radiance that would exit the water traveling toward the zenith when the Sun is at the zenith and there is no atmosphere, i.e., $\hat{\xi}_s = -\hat{n}_h$ and $\hat{\xi}_v = \hat{n}_h$:

$$[L_w]_N^{\text{exact}} = [L_w(\hat{n}_h)]_N = \overline{F}_0 \Re(\hat{n}_h, -\hat{n}_h) \frac{R(-\hat{n}_h)}{Q(\hat{n}_h, -\hat{n}_h)}. \tag{6}$$

The second is the normalized water-leaving radiance that is usually measured at sea, i.e., the radiance propagating toward the zenith, but with the Sun not necessarily at the zenith:

$$[L_w]_N^{\text{field}} = [L_w(\hat{n}_h)]_N = \overline{F}_0 \Re(\hat{n}_h, \hat{\xi}_s) \frac{R(\hat{\xi}_s)}{Q(\hat{n}_h, \hat{\xi}_s)}. \quad (7)$$

Finally, the third is the normalized water-leaving radiance deduced from the measurement of $L_w(\hat{\xi}_v, \lambda)$ by a spaceborne sensor:

$$[L_w]_N^{\text{space}} = [L_w(\hat{\xi}_v)]_N = \overline{F}_0 \Re(\hat{\xi}_v', \hat{\xi}_s) \frac{R(\hat{\xi}_s)}{Q(\hat{\xi}_v', \hat{\xi}_s)}. \quad (8)$$

It is reasonable to refer all $[L_w]_N$ measurements, either from the surface or from space, to the same geometry. This is conventionally taken to be $[L_w]_N^{\text{exact}}$. Thus

$$[L_w]_N^{\text{field}} = \frac{\Re(\hat{n}_h, \hat{\xi}_s)}{\Re(\hat{n}_h, -\hat{n}_h)} \frac{Q(\hat{n}_h, -\hat{n}_h)}{Q(\hat{n}_h, \hat{\xi}_s)} \frac{R(\hat{\xi}_s)}{R(-\hat{n}_h)} [L_w]_N^{\text{exact}}, \quad (9)$$

$$[L_w]_N^{\text{space}} = \frac{\Re(\hat{\xi}_v', \hat{\xi}_s)}{\Re(\hat{n}_h, -\hat{n}_h)} \frac{Q(\hat{n}_h, -\hat{n}_h)}{Q(_v', \hat{\xi}_s)} \frac{R(\hat{\xi}_s)}{R(-\hat{n}_h)} [L_w]_N^{\text{exact}}. \quad (10)$$

Deriving $[L_w]_N^{\text{exact}}$ requires detailed modeling of Q as a function of Sun-viewing geometry and R as a function of the solar zenith angle. For validation of remote measurements of L_w, one wants to compare simultaneous measurements of $[L_w]_N^{\text{field}}$ and $[L_w]_N^{\text{space}}$. These quantities are related through

$$\frac{[L_w]_N^{\text{field}}}{[L_w]_N^{\text{space}}} = \frac{\Re(\hat{n}_h, \hat{\xi}_s)}{\Re(\hat{\xi}_v', \hat{\xi}_s)} \frac{Q(\hat{\xi}_v', \hat{\xi}_s)}{Q(\hat{n}_h, \hat{\xi}_s)}, \quad (11)$$

with no dependence on R or on $\bar{r}$.

The principal focus of the Morel papers was the computation of $R(\hat{\xi}_s)/Q(\hat{\xi}_v', \hat{\xi}_s)$ as a function of the inherent optical properties of the water and through the dependence of the inherent optical properties on the bio-optical properties, e.g., the concentration of chlorophyll a on the bio-optical properties as well. Here we focus on the computation of $\Re(\hat{\xi}_v', \hat{\xi}_s)$. When the water surface is flat, computation of $\Re(\hat{\xi}_v', \hat{\xi}_s)$ poses no difficulty—the Fresnel reflectances are readily computed, and we implicitly assume that R is small enough that multiple reflections within the water can be ignored, or at least cancel in the ratios required in Eqs. (6)–(11). However, this is not the case when the surface is roughened by the wind. Recalling that what we really want in $\Re$ is the solar irradiance transmitted into the water and the upwelling radiance transmitted into the air, we should more appropriately write

$$\Re(\hat{\xi}_v', \hat{\xi}_s) = \left\{ \frac{t_f(\hat{\xi}_v') \bar{t}_f(\hat{\xi}_s)}{m^2[1 - \bar{r}R(\hat{\xi}_s)]} \right\} \quad (12)$$

in place of Eq. (5). When the surface is flat,

$$t_f(\hat{\xi}_v') = 1 - \rho_f(\hat{\xi}_v'), \; \bar{t}_f(\hat{\xi}_s) = 1 - \bar{\rho}_f(\hat{\xi}_s);$$

however, when the surface is roughened by the wind, there is absolutely no relationship between $t_f(\hat{\xi}_v')$ and $1 - \rho_f(\hat{\xi}_v')$ or between $\bar{t}_f(\hat{\xi}_s)$ and $1 - \bar{\rho}_f(\hat{\xi}_s)$. For a collimated beam (sunlight) $\bar{t}_f(\hat{\xi}_s) \cong 1 - \bar{\rho}_f(\hat{\xi}_s)$, and this approximation will usually be good enough for our purposes. However, because the upwelling radiance beneath the water surface is quite diffuse, the relationship $t_f(\hat{\xi}_v') \cong 1 - \rho_f(\hat{\xi}_v')$ can lead to very large errors in $\Re$. These statements are made concrete in Sections 3 and 4.

3. Reciprocity Relationship

Our analysis of radiative transfer across the air–sea interface utilizes the reciprocity principle.[9] Consider a medium (or a portion of a medium) of volume V, bounded by a surface S. Let $\hat{n}$ be the outward normal to S and the interior of V be free of sources. Then Yang and Gordon[10] showed that if V is subjected (separately) to two different radiances incident on its surface, i.e., $L_1(\boldsymbol{\rho}, \hat{\xi})$ and $L_2(\boldsymbol{\rho}, \hat{\xi})$, where $\boldsymbol{\rho}$ is the position vector of points on S and $\hat{\xi} \cdot \hat{n} < 0$,

$$\oint_S dS \int_{\hat{\xi}\cdot\hat{n}<0} |\hat{\xi} \cdot \hat{n}| \left[\frac{L_1(\boldsymbol{\rho}, \hat{\xi}) L_2(\boldsymbol{\rho}, -\hat{\xi})}{m^2(\boldsymbol{\rho})} - \frac{L_1(\boldsymbol{\rho}, -\hat{\xi}) L_2(\boldsymbol{\rho}, \hat{\xi})}{m^2(\boldsymbol{\rho})} \right] d\Omega(\hat{\xi}) = 0, \quad (13)$$

where the integration over $d\Omega(\hat{\xi})$ is only over directions for which $\hat{\xi} \cdot \hat{n} < 0$, i.e., directions for which $\hat{\xi}$ points into the medium ($-\hat{\xi}$ points out of the medium). To apply this to radiative transfer across the air–water interface, we choose V to be a rectangular box with the top just above the interface and the bottom just below. We assume that the horizontal dimension of the box is much larger than the vertical, the water and atmosphere are both transparent, and label points on the top surface by the position vector $\boldsymbol{\rho}_A$ and on the bottom surface by $\boldsymbol{\rho}_B$. The normal to the top surface of the box is $\hat{n}_h$ (Fig. 1), and the normal to the bottom surface is $-\hat{n}_h$. We consider the following two cases (Fig. 2) in Subsections 3.A and 3.B.

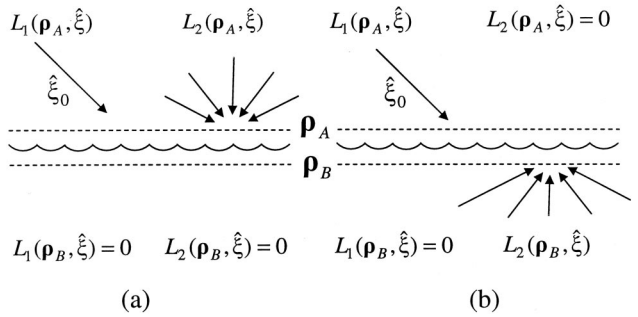

Fig. 2. Schematic illustrating the incident radiances $L_1(\boldsymbol{\rho}, \hat{\xi})$ and $L_2(\boldsymbol{\rho}, \hat{\xi})$ for application of the reciprocity principle to radiative transfer across the air–water interface. (a) Reflects discussion in Subsection 3.A (reflection of uniform radiance incident from above). (b) Reflects discussion in Subsection 3.B (transmittance of radiance incident from below). The normals to the surfaces $\boldsymbol{\rho}_A$ and $\boldsymbol{\rho}_B$ are directed away from the interface. $L_2(\boldsymbol{\rho}_A, \hat{\xi})$ is uniform; $L_2(\boldsymbol{\rho}_B, \hat{\xi})$ is not necessarily uniform.

A. Reflection of Uniform Radiance Incident from Above

Here we take $L_1(\boldsymbol{\rho}_A, \hat{\xi}) = F_0\delta(\hat{\xi} - \hat{\xi}_0)$ for $\hat{\xi}\cdot\hat{n} < 0$ (i.e., a parallel beam of irradiance propagating toward the surface in the direction $\hat{\xi}_0$) and $L_2(\boldsymbol{\rho}_A, \hat{\xi}) = L_0$ for $\hat{\xi}\cdot\hat{n} < 0$ (i.e., a distribution of uniform radiance incident on the surface from above). Furthermore, at the lower surface of the box we have no incident radiance in either problem: $L_1(\boldsymbol{\rho}_B, \hat{\xi}) = L_2(\boldsymbol{\rho}_B, \hat{\xi}) = 0$ for $\hat{\xi}\cdot\hat{n} < 0$. Then Eq. (13) reduces to

$$\frac{L_2(\boldsymbol{\rho}_A, -\hat{\xi}_0)}{L_0} = \frac{\int_{\hat{\xi}\cdot\hat{n}<0} L_1(\boldsymbol{\rho}_A, -\hat{\xi})\,|\hat{\xi}\cdot\hat{n}|\,\mathrm{d}\Omega(\hat{\xi})}{F_0\,|\hat{\xi}_0\cdot\hat{n}|} = \frac{\int_{\hat{\xi}\cdot\hat{n}>0} L_1(\boldsymbol{\rho}_A, \hat{\xi})\,|\hat{\xi}\cdot\hat{n}|\,\mathrm{d}\Omega(\hat{\xi})}{F_0\,|\hat{\xi}_0\cdot\hat{n}|}.$$

The last integral is just the upward irradiance $E_u(\boldsymbol{\rho}_A, \hat{\xi}_0)$ of the incident beam reflected from the surface. Thus

$$\frac{L_2(\boldsymbol{\rho}_A, -\hat{\xi}_0)}{L_0} = \frac{E_{1u}(\boldsymbol{\rho}_A, \hat{\xi}_0)}{F_0\,|\hat{\xi}_0\cdot\hat{n}|}. \tag{14}$$

We define the left-hand side as the reflected radiance in the direction $-\hat{\xi}_0$ when there is uniform radiance incident on the interface from above: $r_+(-\hat{\xi}_0) \overset{\text{def}}{=} L_2(\boldsymbol{\rho}_A, -\hat{\xi}_0)/L_0$.

B. Transmittance of Radiance Incident from Below

Here we take $L_1(\boldsymbol{\rho}_A, \hat{\xi})$ and $L_1(\boldsymbol{\rho}_B, \hat{\xi})$ to be the same as above, but take $L_2(\boldsymbol{\rho}_A, \hat{\xi}) = 0$ for $\hat{\xi}\cdot\hat{n} < 0$, and specify $L_2(\boldsymbol{\rho}_B, \hat{\xi})$ for $\hat{\xi}\cdot\hat{n} < 0$. These lead to

$$L_2(\boldsymbol{\rho}_A, -\hat{\xi}_0) = \frac{\int_{\hat{\xi}\cdot\hat{n}<0} L_1(\boldsymbol{\rho}_B, -\hat{\xi})L_2(\boldsymbol{\rho}_B, \hat{\xi})\,|\hat{\xi}\cdot\hat{n}|\,\mathrm{d}\Omega(\hat{\xi})}{m^2F_0\,|\hat{\xi}_0\cdot\hat{n}|} = \frac{\int_{\hat{\xi}\cdot\hat{n}>0} L_1(\boldsymbol{\rho}_B, \hat{\xi})L_2(\rho_B, -\hat{\xi})\,|\hat{\xi}\cdot\hat{n}|\,\mathrm{d}\Omega(\hat{\xi})}{m^2F_0\,|\hat{\xi}_0\cdot\hat{n}|}. \tag{15}$$

If $L_2(\boldsymbol{\rho}_B, \hat{\xi})$ is uniform, i.e., L_0, and removed from the integral, the integration produces the downward irradiance at $\boldsymbol{\rho}_B$ from the collimated beam:

$$E_{1d}(\boldsymbol{\rho}_B, \hat{\xi}_0) = \int_{\hat{\xi}\cdot\hat{n}>0} L_1(\boldsymbol{\rho}_B, \hat{\xi})\,|\hat{\xi}\cdot\hat{n}|\,\mathrm{d}\Omega(\hat{\xi}).$$

Therefore

$$t_-(-\hat{\xi}_0) \overset{\text{def}}{=} m^2\frac{L_2(\boldsymbol{\rho}_A, -\hat{\xi}_0)}{L_0} = \frac{E_{1d}(\boldsymbol{\rho}_B, \hat{\xi}_0)}{F_0\,|\hat{\xi}_0\cdot\hat{n}|},$$

where $t(-\hat{\xi}_0)$ is the transmitted radiance into the direction $-\hat{\xi}_0$ when the interface is illuminated from below with uniform radiance. However, since

$$E_{1u}(\boldsymbol{\rho}_A, \hat{\xi}_0) + E_{1d}(\boldsymbol{\rho}_B, \hat{\xi}_0) = F_0\,|\hat{\xi}_0\cdot\hat{n}|,$$

we have that

$$r_+(-\hat{\xi}_0) + t_-(-\hat{\xi}_0) = 1, \tag{16}$$

i.e., across the air–water interface the sum of the transmittance of uniform radiance incident from below and the reflectance of uniform radiance incident from above into a given direction is unity. Note that in Eq. (16), $-\hat{\xi}_0$ is the propagation direction after reflection from or transmission through the interface. If we reverse the positions of $F_0\delta(\hat{\xi} - \hat{\xi}_0)$ and L_0 above and in Subsection 3.A, it should be clear that

$$r_-(-\hat{\xi}_0) + t_+(-\hat{\xi}_0) = 1,$$

i.e., across the air–water interface the sum of the transmittance of uniform radiance incident from above and the reflectance of uniform radiance incident from below into a given direction is unity.

4. Computation of t_f and $\bar{t}_f$ in $\Re$

Computation of $\bar{t}_f$ is simple: It is just the Fresnel transmittance of the irradiance of a collimated beam

across the air–water interface. Computation of t_f is effected by use of Eq. (15) directly. However, in the past t_f has been computed with the assumption that the upwelling radiance just beneath the interface is uniform. For completeness, we use both approaches and show that they lead to similar results.

A. Computation of $\Re$ with Equation (15)

For a surface roughened by the wind, $L_1(\boldsymbol{\rho}_B, \hat{\xi})$ is small except for directions near $\hat{\xi}_0'$, the direction of propagation of the refracted collimated beam through a flat surface. Experimentally, it is known that the subsurface upwelling radiance distribution $L_2(\boldsymbol{\rho}_B, -\hat{\xi})$, although not uniform, is a slowly varying function of $-\hat{\xi}$. Thus we can simplify the integration by expanding the subsurface radiance in a power series:

$$L_2(\boldsymbol{\rho}_B, -\hat{\xi}) = L_2(\boldsymbol{\rho}_B, -\hat{\xi}_c) + (-\hat{\xi} + \hat{\xi}_c)[\nabla L_2(\boldsymbol{\rho}_B, -\hat{\xi})]_{\hat{\xi}=\hat{\xi}_c} + \frac{1}{2}(-\hat{\xi} + \hat{\xi}_c)^T[\mathbf{H}]_{\hat{\xi}=\hat{\xi}_c}(-\hat{\xi} + \hat{\xi}_c) + \ldots, \tag{17}$$

where $\mathbf{H}$ is the Hessian matrix (the matrix of the second derivatives of L_2). The vector $(-\hat{\xi} + \hat{\xi}_c)^T$ is the transpose of the column vector $(-\hat{\xi} + \hat{\xi}_c)$, and $-\hat{\xi}_c$ is yet to be determined. If we choose

$$\hat{\xi}_c = \frac{\int_{\hat{\xi}\cdot\hat{n}>0} \hat{\xi} L_1(\boldsymbol{\rho}_B, \hat{\xi})\,|\hat{\xi}\cdot\hat{n}|\,\mathrm{d}\Omega(\hat{\xi})}{\int_{\hat{\xi}\cdot\hat{n}>0} L_1(\boldsymbol{\rho}_B, \hat{\xi})\,|\hat{\xi}\cdot\hat{n}|\,\mathrm{d}\Omega(\hat{\xi})}, \tag{18}$$

then, when the series is inserted into Eq. (15), the gradient term will integrate to zero; and, ignoring the third- and higher-order terms in Eq. (17), we have

$$L_2(\boldsymbol{\rho}_A, -\hat{\xi}_0) = L_2(\boldsymbol{\rho}_B, \hat{\xi}_c) \times \frac{\int_{\hat{\xi}\cdot\hat{n}>0} L_1(\boldsymbol{\rho}_B, \hat{\xi})\,|\hat{\xi}\cdot\hat{n}|\,\mathrm{d}\Omega(\hat{\xi})}{m^2 F_0\,|\hat{\xi}_0\cdot\hat{n}|},$$

but the integral is the downwelling irradiance just beneath the surface with collimated illumination, i.e.,

$$E_{1d}(\hat{\xi}_0) = \int_{\hat{\xi}_q\cdot\hat{n}>0} L_1(\boldsymbol{\rho}_B, \hat{\xi})\,|\hat{\xi}\cdot\hat{n}|\,\mathrm{d}\Omega(\hat{\xi}).$$

Therefore

$$m^2 \frac{L_2(\boldsymbol{\rho}_A, -\hat{\xi}_0)}{L_2(\boldsymbol{\rho}_B, -\hat{\xi}_c)} = \frac{E_{1d}(\hat{\xi}_0)}{F_0\,|\hat{\xi}_0\cdot\hat{n}|} \overset{\text{def}}{=} t_f(\hat{\xi}_0), \tag{19}$$

where $t_f(\hat{\xi}_0)$ is just the transmittance of the irradiance of a parallel beam, incident from above propagating in a direction $\hat{\xi}_0$, across the interface.

Actual computation of $t_f(\hat{\xi}_0)$ and $\hat{\xi}_c$ requires knowledge of the surface roughness. Modeling the sea surface as a collection of individual facets, Cox and Munk[11] determined the distribution of facet normals required to explain the Sun's glitter pattern (as a function of wind speed) observed from high altitude. Preisendorfer and Mobley[12] used this distribution to develop realizations of the sea surface for which propagation across the interface could be studied by Monte Carlo techniques (see also Mobley[13]). For a water surface illuminated with irradiance propagating in a direction $\hat{\xi}_0$, they computed the irradiance reflectance as a function of wind speed. Since irradiance is conserved across the air–water interface, this reflectance is just $1 - t_f(\hat{\xi}_0)$ in Eq. (19), and the transmittances we desire can be determined from their results. For wind speeds $0 < W < 20$ m/s, they found that $t_f(\hat{\xi}_0)$ differs from $T_f(\hat{\xi}_0)$, the Fresnel transmittance for a flat interface, by less that 0.01 for $0 \le \theta_0 \le 60°$, where θ_0 is the incident angle $\theta_0 = \arccos(|\hat{\xi}_0\cdot\hat{n}|)$, i.e., the angle between $\hat{\xi}_0$ and the downward normal at the surface. For larger values of θ_0, they provide graphs from which the decrease in $t_f(\hat{\xi}_0)$ with increasing wind speed can be estimated. Other models of reflection from a wind-roughened surface (e.g., Haltrin[14] who used the wave energy spectrum rather than the Cox and Munk surface slope distribution to create realizations of the water surface) yield similar conclusions for $\theta_0 < 60°$.

The vector $\hat{\xi}_c$ about which the subsurface radiance is expanded is easy to find from its definition. The simplest case to examine is that for an omnidirectional wind. In this case, $\hat{\xi}_c$ is in the plane of $\hat{\xi}_0$ and $\hat{n}$, and its position is given by the angle with respect to the normal $\theta_c = \arccos(|\hat{\xi}_c\cdot\hat{n}|)$. This angle is close to the refracted angle in the water when the sea surface is flat, i.e., $\theta_0' = \arccos(|\hat{\xi}_0'\cdot\hat{n}|)$, but slightly larger (Fig. 3). It can even be larger than the critical angle $\theta_v' = \arcsin(1/m) \cong 48.2°$.

It remains to consider the higher-order terms in Eq. (17). Using radiance distributions computed[8] for low and medium concentrations of chlorophyll a, I computed $\mathbf{H}$ and evaluated the appropriate integrals [Eq. (17)] for wind speeds of 8 and 16 m/s, $\theta_s = 60°$, and chlorophyll a concentrations of 0.1 and 1.0 mg/m^3. For these cases, the Hessian term in Eq. (17) contributed $<0.5\%$ of the leading term and thus can be safely ignored. Therefore, with these changes, i.e., restricting θ_s and θ_v to be less than 60°, $\bar{t}_f(\hat{\xi}_s) \cong T_f(\hat{\xi}_s)$ and $t_f(\hat{\xi}_v) \cong T_f(\hat{\xi}_v)$, and the normalized water-leaving radiance becomes

$$[L_w(\hat{\xi}_v)]_N = \overline{F}_0 \Re(\hat{\xi}_v, \hat{\xi}_s) \frac{R(\hat{\xi}_s)}{Q(\hat{\xi}_c, \hat{\xi}_s)},$$

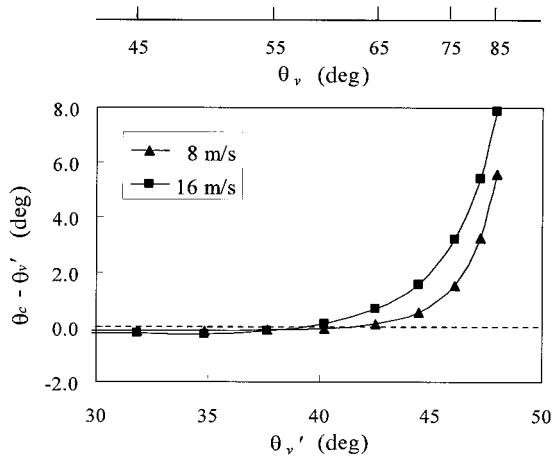

Fig. 3. Difference between the true viewing angle θ_c and the viewing angle for a flat surface θ_v' as a function of wind speed. The upper scale is the viewing angle θ_v (above the surface). Note that θ_c can be greater than the critical angle for a flat surface.

where

$$\Re(\hat{\xi}_v, \hat{\xi}_s) = \left\{ \frac{T_f(\hat{\xi}_v) T_f(\hat{\xi}_s)}{m^2[1 - \bar{r}R(\hat{\xi}_s)]} \right\},$$

where T_f is the Fresnel transmittance for a flat air–water interface, and $\hat{\xi}_c$ differs only slightly from $\hat{\xi}_v'$ (Fig. 3).

B. Computation of $\Re$ Assuming $L_u(\boldsymbol{\rho}_B, \hat{\xi})$ is Uniform

The conclusions regarding $\bar{t}_f(\hat{\xi}_s)$ remain the same as above. However, now we compute $t_f(\hat{\xi}_v)$ using Eq. (16). Austin[3] provides computations of $r_+(-\hat{\xi}_0)$ for a rough surface following the Cox–Munk[11] facet normal distribution. Figure 4 provides the resulting $t_-(\hat{\xi}_v) = t_-(-\hat{\xi}_0)$ as a function of $\theta_v = \arccos(|\hat{\xi}_v \cdot \hat{n}|)$. Again, the conclusion is that $t_f(\hat{\xi}_v) \cong T_f(\hat{\xi}_v)$ for $\theta_v \leq 60°$.

C. Example of the Resulting $\Re$

An example of $\Re$ resulting from the computations above is now provided. I make the same assumptions and approximations as made by Morel and Gentili[7] in preparing their Fig. 11. These assumptions are that $\bar{t}_f(\hat{\xi}_s)$ can be replaced by 0.957 with an error less than $\pm 3\%$, $1 - \bar{r}R(\hat{\xi}_s)$ can be replaced by $0.985 \pm 1.5\%$ when $0 \leq R \leq 0.06$, and $m = 1.341$. Using these, and our present development of $t_f(\hat{\xi}_v)$, $\Re(\theta_v, \theta_s)$ as a function of the viewing angle (above the surface) is provided in Fig. 5 (solid curves). The dashed curves in Fig. 5 are computed as in Morel and Gentili.[7] It can be seen that use of the Morel and Gentili development for $\Re(\theta_v, \theta_s)$ could lead to significant error for large viewing angles and wind speeds. For example, when we derive $[L_w]_N^{\text{exact}}$ from $[L_w]_N^{\text{space}}$, the result could range from 13 to 25% too high at a viewing angle of 60°. This can be circumvented by use of the Morel and Gentili results for a wind speed of 0.

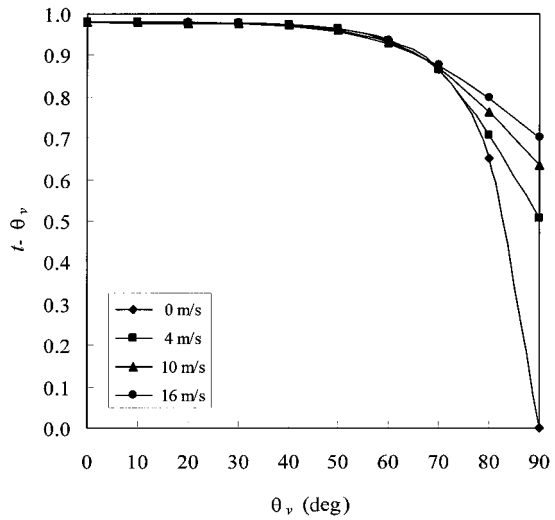

Fig. 4. $t_-(\theta_v)$, the transmittance of uniform radiance incident from below the air–water interface, as a function of wind speed computed with the Cox and Munk[11] probability distribution of the wave facet normal.

5. Concluding Remarks

I have shown that the influence of surface roughness on the transfer of subsurface radiance through the air–water interface is minimal, i.e., for surface viewing angles and solar zenith angles $\leq 60°$, the transmittances can be replaced by the Fresnel transmittances for a flat surface with an error in transmittance of ≤ 0.01. Thus the large variations in $\Re$ with wind speed (up to 40%) shown in Morel *et al.*[8] (their Fig. 4) and Morel and Gentili[7] (their Fig. 11) are not realistic, and a wind speed of zero is appropriate for $0 \leq \theta_v \leq 60°$. However, the angle at which the upwelling below-surface radiance is to be related to the surface above-surface radiance is θ_c, not θ_v'.

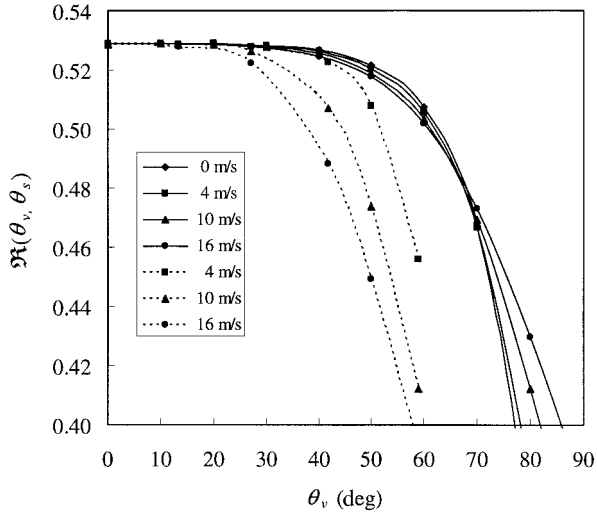

Fig. 5. $\Re(\theta_v, \theta_s)$ as a function of wind speed computed with the Cox and Munk[11] probability distribution of the wave facet normal (solid curves). The dashed curves are from Morel and Gentili[7] (their Fig. 11). As in Morel and Gentili, I suppressed any dependence on θ_s by using mean values for $\bar{t}_f(\xi_s)$ and $1 - \bar{r}R(\xi_s)$.

The error made in Refs. 7 and 8 was in relating the reflectance of uniform radiance from below rather than from above to $t_f(\theta_v)$. This leads to the dashed curves in Fig. 5. This likely resulted from the Gordon and Clark[1] use of $(1 - \rho_f)$'s in Eq. (2) rather than the more-explicit t_f's. It should be noted here that validity of the principal focus in the papers by Morel and co-workers (the computation of bidirectional affects in R/Q) is unaffected by the incorrect computation of $\Re$.

Appendix A: Confirmation of the Present Analysis by Morel and Gentili

Upon being informed that my use of the reciprocity principle to compute $\Re$ yielded results that were in contradiction to their original computations, Morel and Gentili reformulated their analysis of the interaction of light with a rough surface and confirmed the results presented here. Morel supplied me with the following discussion for inclusion in this paper.

When producing the $\Re(\theta_v, \theta_s)$ values, Morel and Gentili[7] actually made a direct use of the tabulated values in Austin[3] (as displayed in Fig. 4). To test these values and improve the interpolation, they also operated a Monte Carlo model. The photons were generated inside the water along a given θ' direction, impinging the rough surface (modeled according to the Cox and Munk slope distribution); then the Fresnel internal reflectance for each photon was computed. The sum of these reflectances, once they are weighted according to the probability of their occurrence, provides the answer. This way of computing assumes a uniform distribution of the upward radiance field [and thus contradicts Eq. (4) where the Q-factor expresses the nonuniformity of this field and its dependence on the solar position]. Apart from this assumption, which has a minor effect, the computation is exact when the energy that remains inside the water body, because of these backward reflections, is to be assessed. It is not correct, however, for the remote-sensing problem, except if the sea is level.

Indeed, in such a simulation the photons emerging from the water diverge within an angular domain, the width of which depends on the wave slope variance. In other words, these photons are traveling in air in various directions centered on $\hat{\xi}_v$, but not uniquely in this direction oriented toward the sensor. A backward Monte Carlo technique can solve the problem as it is posed. The photons are now generated along the $-\hat{\xi}_v$ direction; they enter the water through the wavy interface and are refracted (again within a cone, yet narrower than the previous one in air because of the refraction). To each of these refracted directions corresponds a specified internal reflectance. Their weighted sum represents the desired quantity. In this computation, the upward radiance field is also considered as uniform.

By using these averaged internal reflectances, the $\Re$ values are deeply modified for a large θ_v domain compared with those previously obtained. They exactly coincide with those produced by Eq. (16) and displayed in Fig. 5. Note that ignoring the anisotropy of the upward radiance field is of a second-order effect on the resulting $\Re$ values.

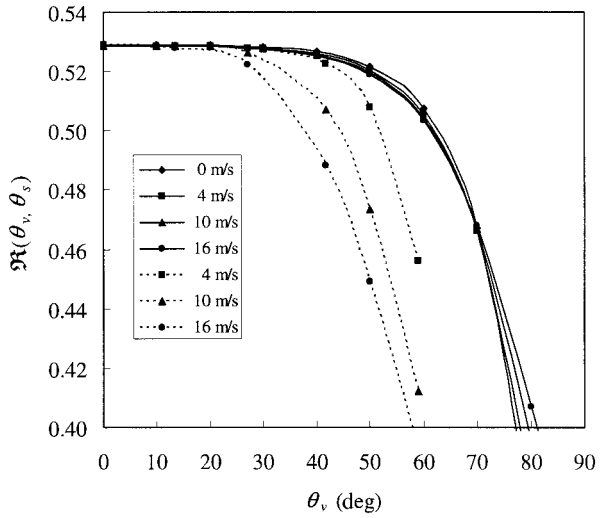

Fig. 6. $\Re(\theta_v, \theta_s)$ as a function of wind speed recomputed by Morel and Gentili (as described in Appendix A) with the Ebuchi and Kizu[15] probability distribution of the wave facet normal (solid curves). The dashed curves are from Morel and Gentili[7] (their Fig. 11).

The (Gaussian) probability distribution of surface slope as a function of wind speed has been recently revisited, based on approximately 30×10^6 satellite observations.[15] A narrower slope distribution and a lower sensitivity to the wind direction (compared with those in the Cox and Munk[11] study) seems to be more realistic. These probability functions have been used in the same way (backward Monte Carlo), and they result in similar $\Re$ values, except that the influence of the wind speed is notably reduced (Fig. 6). From a practical viewpoint, this is an important advantage as a unique relationship between $\Re(\theta_v, \theta_s)$ and θ_v, independent from the wind speed, could be safely used without loss of accuracy, at least for viewing angles up to 70°.

This research was initiated by a comment to the author by R. E. Evans that when the accepted relationships for the bidirectional affects on water-leaving radiance were employed with the moderate resolution imaging spectroradiometer (MODIS) imagery, the resulting normalized water-leaving radiance showed significant (and unrealistic) variation at large viewing angles. The author benefited from conversations with K. J. Voss and M. Wang and is grateful to André Morel for the confirmation provided in Appendix A. This research received support from the National Aeronautics and Space Administration under contracts NAS5-31363 and NNG04HZ21C.

References

1. H. R. Gordon and D. K. Clark, "Clear water radiances for atmospheric correction of coastal zone color scanner imagery," Appl. Opt. **20,** 4175–4180 (1981).
2. H. R. Gordon, O. B. Brown, R. H. Evans, J. W. Brown, R. C.

Smith, K. S. Baker, and D. K. Clark, "A semi-analytic radiance model of ocean color," J. Geophys. Res. **93D,** 10909–10924 (1988).
3. R. W. Austin, "The remote sensing of spectral radiance from below the ocean surface," in *Optical Aspects of Oceanography*, N. G. Jerlov and E. S. Nielsen, eds. (Academic, London, 1974), pp. 317–344.
4. A. Morel and B. Gentili, "Diffuse reflectance of oceanic waters: its dependence on Sun angle as influenced by the molecular scattering contribution," Appl. Opt. **30,** 4427–4438 (1991).
5. A. Morel and B. Gentili, "Diffuse reflectance of oceanic waters. II. Bidirectional aspects," Appl. Opt. **32,** 6864–6879 (1993).
6. A. Morel, K. J. Voss, and B. Gentili, "Bidirectional reflectance of oceanic waters: a comparison of modeled and measured upward radiance fields," J. Geophys. Res. **100C,** 13143–13150 (1995).
7. A. Morel and B. Gentili, "Diffuse reflectance of oceanic waters. III. Implication of bidirectionality for the remote sensing problem," Appl. Opt. **35,** 4850–4862 (1996).
8. A. Morel, D. Antoine, and B. Gentili, "Bidirectional reflectance of oceanic waters: accounting for Raman emission and varying particle scattering phase function," Appl. Opt. **41,** 6289–6306 (2002).
9. K. M. Case, "Transfer problems and the reciprocity principle," Rev. Mod. Phys. **29,** 651–663 (1957).
10. H. Yang and H. R. Gordon, "Remote sensing of ocean color: assessment of the water-leaving radiance bidirectional effects on the atmospheric diffuse transmittance," Appl. Opt. **36,** 7887–7897 (1997).
11. C. Cox and W. Munk, "Measurements of the roughness of the sea surface from photographs of the Sun's glitter," J. Opt. Soc. Am. **44,** 838–850 (1954).
12. R. W. Preisendorfer and C. D. Mobley, "Albedos and glitter patterns of a wind-roughened sea surface," J. Phys. Oceanogr. **16,** 1293–1316 (1986).
13. C. D. Mobley, *Light and Water: Radiative Transfer in Natural Waters* (Academic, New York, 1994).
14. V. I. Haltrin, "Algorithm and code to calculate specular reflection of light from a wavy water surface," in *Proceedings of the Seventh International Conference on Remote Sensing for Marine and Coastal Environments* (Veridian, Ann Arbor, Mich., 2002), pp. 1–7.
15. N. Ebuchi and S. Kizu, "Probability distribution of surface slope derived using sun glitter images from geostationary meteorological satellite and surface vector winds from scatterometers," J. Oceanogr. **58,** 477–486 (2002).